УДК 624.048-033.26:621.651

M. Demchuk

VERIFICATIONS OF GROUTING MODELS

Calculation errors are estimated within the framework of a model of the standard injection test. Such the test is conducted to verify simplifying assumptions of the model through comparison of model calculations with respective laboratory measurements. It is shown that the verification presented in this work as well as similar verifications presented in recent research, provides a small amount of information.

Keywords: error due to uncertainties in input data, truncation error, round off error, numerical solution analysis, uncertainty uniformity principle.

Introduction. Before creations of foundations on weak soil plots, to make better elastic properties of soil tracts the grouting operations are performed. In this technique a cement grout is injected under high pressure into a porous medium that can be water saturated or dry. The aim is reached after the grout hardening [7, p. 227]. The process of cement grout propagation in a soil is complicated by the fact that the infiltrate is composed of particles. It gives rise to the phenomenon called the deep bed filtration or the depth filtration. Depending on particle and pore throat sizes, two limiting cases are distinguished in the description of this phenomenon. In the first case, large particles get stuck in small pore throats. It entails a decrease in "the area allowed for a fluid flow". Whereas in the second case, small particles create the precipitate on large pore bodies and large pore throats that results in slow decreases of pore throat sizes [9, p. 1637].

Grouting is rather costly and time consuming. Its regime is determined by the concentration distribution evolution [6, p. 1195]. Therefore, a calculation of this evolution using mathematical modeling is important.

Various simplifying assumptions were verified through the standard laboratory test [6; 7]. The set up of this test is the following. A cement grout is injected in the base of a vertical tube opened at the top and filled with a water saturated sand at a constant pumping rate. A comparison of model calculations with laboratory measurements verifies the set of assumptions used in a model formulation. An amount of information it provides depends upon values of uncertainties in compared quantities [2, p. 47]. There are three types of numerical calculation errors: an error due to uncertainties in input data, a round off error, and a truncation error [3, p. 11–13]. If input data are fixed, then the error of the first type is zero. If the finite difference scheme according to which the calculations are performed is conditionally stable, then the round off error is negligible. This property of the scheme is usually verified during a numerical solution analysis. Usually, the main contribution to a method error comes from an approximation error. In the case of the above mentioned test modeling, an estimation of the approximation errors is complicated by the fact that at any moment of time the functions being sought contain the high gradient regions that correspond to the transition from a soil with the maximal cement concentration to the soil with the zero one. According to the uncertainty uniformity principle [5, p. 35], to estimate these errors properly calculations on time layers should be performed on non-uniform grids with smaller space increments inside such regions and larger ones outside of them. In our case, positions of these high gradient regions are changing with time and not known in advance. Therefore, in existing models of the standard laboratory test calculation errors are not estimated [8, p. 79].

One of the models of the above mentioned standard laboratory test is presented in paper [2, p. 49–50]. In this model, boundary conditions conform to initial ones. The results of laboratory measurements performed during the standard test and the method of a proper treatment of high gradient regions in sought functions during numerical calculations according to the model in hand are presented in [8, p. 79–81; p. 88–90]. The aim of this work consists in estimating the errors of calculations according to this model that are to be compared with these laboratory measurements.

The Grouting Model Under Consideration. We assume that the coordinate origin is chosen at the injection point and that the coordinate axis is directed upward. In this work we use the following notations. ε is a small positive parameter, α_0 and α_1 are large positive parameters. They are introduced in the model to conform initial conditions with boundary ones, and their values will be obtained later in the result of the analysis of the numerical solutions. $I = (-\varepsilon, L)$ is an interval (a set

of points (x): $x \in (-\varepsilon, L)$). $I_T = I \times (0, T)$ is a rectangle (a set of points (x, t): $(x) \in I$, $t \in (0, T)$), $A_{T,1}$ is the bottom side of I_T (a set of points $(-\varepsilon, t)$: $t \in [0, T]$), $A_{T,2}$ is the top side of I_T (a set of points (L, t): $t \in [0, T]$), $p(x,t)$ and $c(x,t)$ denote the pore fluid pressure and the grout concentration respectively. K is the permeability of the medium, m is the medium porosity, ρ is the fluid phase density, g is the acceleration of free fall, μ_1 and c_{imp} are the grout viscosity and the grout concentration inside the injector respectively, μ_2 is the water viscosity. a_L is the longitudinal dispersion coefficient, D^* is the diffusion coefficient, $\mu = (\mu_1 - \mu_2)c/c_{\text{imp}} + \mu_2$, $D_h = a_L V + D^*$, $V = -K(\partial p/\partial x + \rho g)/\mu/m$. $f_\theta(\alpha \cdot x)$ is the function that tends to the function

$$\theta(x) = \begin{cases} 0, & if\ x < 0, \\ 1/2, & if\ x = 0, \\ 1, & if\ x > 0, \end{cases} \quad (1)$$

with $\alpha \to +\infty$. S is the area of the interface between the injector and the porous medium, L is the tube length, $\mu_{L,0} = (\mu_1 - \mu_2)(1 - f_\theta(\alpha_0 L)) + \mu_2$, $\mu_{0,0} = (\mu_1 - \mu_2) \times (1 - f_\theta(-\alpha_0 \varepsilon)) + \mu_2$, $V_{L,0} = \mu_1 V_0 (1 - f_\theta(\alpha_1 x) - x df(\alpha_1 x)/dx)_{x=L}/\mu_{L,0}$, $V_0 = q_{\text{imp}}/S/m$.

In paper [2, p. 49–50], the mathematical model of the standard laboratory test described in the previous section with boundary conditions conforming to initial ones has been formulated. In it the ground skeleton is regarded as absolutely rigid and the depth filtration is not taken into account. This model is the following system of two partial differential equations valid for such values x and t that $(x, t) \in I_T$

$$m\partial c/\partial t = -mV \cdot \partial c/\partial x + \partial(mD_h \cdot \partial c/\partial x)/\partial x, \quad (2)$$

$$m\beta_p(\partial p/\partial t + V\partial p/\partial x) - \partial(K(\partial p/\partial x + \rho g)/\mu)/\partial x = 0 \quad (3)$$

with such initial conditions valid if $t = 0$ and $x \in \bar{I}$

$$p = \rho g(L - x) + \mu_1 m V_0 x(f_\theta(\alpha_1 x) - 1)/K, \quad (4)$$

$$\tilde{c} = (1 - f_\theta(\alpha_0 x)) \cdot c_{\text{imp}} \quad (5)$$

and boundary conditions

$$\partial p/\partial x = -\mu_1 m V_0 (1 - f_\theta(\alpha_1 x) - x df_\theta(\alpha_1 x)/dx)/K - \rho \cdot g, \quad (6)$$

$$c = c_{\text{imp}}(1 - f_\theta(-\alpha_0 \varepsilon)) \quad (7)$$

where $(x, t) \in A_{T,1}$ and

$$p = \mu_1 m V_0 L(f_\theta(\alpha_1 L) - 1)/K, \quad (8)$$

$$\partial c/\partial x = -c_{\text{imp}}(df_\theta(\alpha_0 x)/dx)(a_L V_{L,0} + D^*)/(a_L V + D^*) \quad (9)$$

where $(x, t) \in A_{T,2}$.

As it is described in paper [8, pp. 88–90], to estimate the model calculation errors properly we need to use two methods to find the numerical solution of problem (2)–(9). In the first one, problem (2)–(9) is discretized at once, while in the second one, we are looking for the numerical solution in the form $p(x,t) = p^{(0)}(x,t) + p^{(1)}(x,t)$, $c(x,t) = c^{(0)}(x,t) + c^{(1)}(x,t)$ where functions $p^{(0)}(x,t)$ and $c^{(0)}(x,t)$ are modeling respectively the evolution of the high gradient region of fluid phase pressure and the evolution of the high gradient region of cement concentration in the fluid phase. We assume (assumption #1) that

$$p^{(0)}(x,t) = \tilde{p}_1(x,t) + f_\theta(\alpha_p(x - V_1 t))(\tilde{p}_2(x,t) - \tilde{p}_1(x,t)), \quad (10)$$

$$c^{(0)}(x,t) = [1 - f_\theta(\alpha_c(x - V_1 t))] \cdot c_{imp} \quad (11)$$

where here and bellow $V_1 = V_0 - K\rho g/\mu_{eff}$,

$$\tilde{p}_2 = (\mu_2 m V_1/K + \rho g)(L - x),$$

$$\tilde{p}_1 = (L - V_1 t)(\rho g + \mu_2 m V_1/K) - (\rho g + \mu_1 m V_{eff}/K)(x - V_1 t).$$

In turn, constants α_c and α_p are defined below. Performing calculations by the second method we assume (assumption #2) that calculation results obtained when $\mu_{eff} = (\mu_1 + \mu_2)/2$ and $V_{eff} = (V_0 + V_1)/2$ do not sufficiently deviate from ones obtained when $\mu_{eff} = \sqrt{\mu_1 \cdot \mu_2}$ and $V_{eff} = \sqrt{V_0 \cdot V_1}$.

To find the numerical solution of problem (2)–(9) we cover $\bar{I}_T$ with uniform grid $\Omega_{N,M} = \{(x_i, t_j), x_i = -\varepsilon + i \cdot h, i = \overline{0,N};\ t_j = j \cdot \tau, j = \overline{0,M}\}$ where $h = (L + \varepsilon)/N$ and $\tau = T/M$. Performing an analysis of numerical solutions of problem (2)–(9), one can use respectively such the measures of the differences between two space distributions of the cement concentration or the pore fluid pressure at a chosen moment of time t $f_1(x,t)$, $f_2(x,t)$ and between two dependencies of the injection pressure on time $g_1(t)$, $g_2(t)$

$$\varepsilon(t)=\max_{x\in[-\varepsilon,\,L]}\left|f_1(x,t)-f_2(x,t)\right|,\quad \omega=\max_{t\in[0,\,T]}\left|g_1(t)-g_2(t)\right|. \quad (12)$$

We denote the measure of the difference between the space distribution of the cement concentration (the pore fluid pressure) at a given moment of time obtained by the second method on grid $\Omega_{2N_1,2N_2}$ and the one obtained by the second method on grid Ω_{N_1,N_2} as ε_1^c $\left(\varepsilon_1^p\right)$. We denote the measure of the difference between the space distribution of the cement concentration (the pore fluid pressure) at a given moment of time obtained by the first method on grid $\Omega_{2N_1,2N_2}$ and the one obtained by the second method on the same grid $\Omega_{2N_1,2N_2}$ as ε_2^c $\left(\varepsilon_2^p\right)$. α_c present in (11) is the solution of the following equation

$$1-f_\theta\left(8\cdot a_L\cdot\alpha_c\right)=1/e^r \quad (13)$$

where r is such that $r>\ln(2)$. Calculating α_c from (13), ideally, we have to use such the value of r at which ratios $\varepsilon_2^c/\varepsilon_1^c$ and $\varepsilon_2^p/\varepsilon_1^p$ are maximal. Performing calculations by the second method we assume that if the order of magnitude of the value of α_p in the right hand side of (10) is the same as the order of magnitude of the value of α_c in the right hand side of (11), then the numerical solution is not sensitive to the choice of the value of α_p (assumption # 3). Therefore, in what follows we assume that $\alpha_p=\alpha_c$.

A Resolution Method. In this section the differential schemes are written in the same form for both methods. In formulas of this section we assume that in the case of the first method $p^{(0)}(x,t)=0$, $c^{(0)}(x,t)=0$ and in the case of the second one $p^{(0)}(x,t)$ and $c^{(0)}(x,t)$ are given by (10) and (11) respectively. Also in these formulas c_i^j and p_i^j where $i=\overline{0,N}$, $j=\overline{0,M}$ denote $c(x_i,t_j)$ and $p(x_i,t_j)$ in the case of the first method and $c^{(1)}(x_i,t_j)$ and $p^{(1)}(x_i,t_j)$ in the case of the second one respectively. In this work we use the following discretization of (2)

$$\mathrm{T}_i^j-\sigma\left(-V_i^j+a_L\left(V_{i+1}^j-V_{i-1}^j\right)/2/h\right)\mathrm{X}_i^{j+1}-\left(D_h\right)_i^j\sigma_1\Lambda_i^{c,j+1}=w_i^j \quad (14)$$

where

$$V_i^j=-K\left(\left(p_{i+1}^j-p_{i-1}^j\right)/2/h+\left(\partial p^{(0)}/\partial x\right)_i^j+\rho g\right)\Big/m/\mu_i^j,$$

$$\mathrm{X}_i^{j+1}=\left(c_{i+1}^{j+1}-c_{i-1}^{j+1}\right)/2/h,$$

$$\mu_i^j=\left(\mu_1-\mu_2\right)\left(c_i^j+\left(c^{(0)}\right)_i^j\right)+\mu_2,$$

$$\Lambda_i^{c,j+1}=\left(c_{i+1}^{j+1}-2c_i^{j+1}+c_{i-1}^{j+1}\right)/h^2,\ \mathrm{T}_i^j=\left(c_i^{j+1}-c_i^j\right)/\tau,$$

$$w_i^j=\left(-V_i^j+a_L\frac{V_{i+1}^j-V_{i-1}^j}{2h}\right)\left(\frac{\partial c^{(0)}}{\partial x}\right)_i^j+\left(D_h\right)_i^j\left(\frac{\partial^2 c^{(0)}}{\partial x^2}\right)_i^j-\left(\frac{\partial c^{(0)}}{\partial t}\right)_i^j+\Omega_i^j, \quad (15)$$

$$\Omega_i^j=(1-\sigma)\left(-V_i^j+a_L\left(V_{i+1}^j-V_{i-1}^j\right)/2/h\right)\cdot\mathrm{X}_i^j+\left(D_h\right)_i^j(1-\sigma_1)\cdot\Lambda_i^{c,j},$$

and the following discretizations of (5), (7), and (9)

$$c_i^0=\widehat{c}_i,\ c_0^{j+1}=\tilde{c}^j,\ \left(c_{N-2}^{j+1}-4c_{N-1}^{j+1}+3c_N^{j+1}\right)/2/h=d^{c,j} \quad (16)$$

where

$$\widehat{c}_i=\left(1-f_\theta\left(\alpha_0\left(-\varepsilon+i\cdot h\right)\right)\right)\cdot c_{imp}-\left(c^{(0)}\right)_i^0, \quad 17)$$

$$\tilde{c}^j=\left(1-f_\theta\left(-\alpha_0\varepsilon\right)\right)c_{imp}-\left(c^{(0)}\right)_0^j, \quad (18)$$

$$d^{c,j}=-\left(a_LV_{L,0}+D^*\right)\Big/\left(a_LV_N^j+D^*\right)c_{imp}\,df_\theta(\alpha_0x)/dx\big|_{x=L}-\left(dc^{(0)}/dx\right)_N^j, \quad (19)$$

$$V_N^j=-K\left(\left(p_{N-2}^j-4p_{N-1}^j+3p_N^j\right)/2/h+\left(\partial p^{(0)}/\partial x\right)_N^j+\rho g\right)\Big/m/\mu_N^j.$$

In (14) $i=1,2,\ldots N-1$, $j=0,1,\ldots M-1$, and in (16) $i=0,1,\ldots N-1$, $j=0,1,\ldots M-1$.

If $\sigma_1\neq 0$, then the system of equations (14), (16) in finite differences can be solved by the "progonka" method [1, p. 276]. If $\sigma_1=0$, then calculations are performed by using the first method. In this case, from (14) it follows that

$$c_i^{j+1}=c_i^j+\tau\sigma\left(-V_i^j+a_L\left(V_{i+1}^j-V_{i-1}^j\right)/2/h\right)\left(c_{i+1}^{j+1}-c_{i-1}^{j+1}\right)/2/h+\tau\cdot w_i^j$$

where w_i^j is calculated according to (15) and $i=1,2,\ldots N-1$, $j=0,1,\ldots M-1$. From the second and the third of equations (16), it follows that

$$c_0^{j+1}=\left(1-f_\theta\left(-\alpha_0\varepsilon\right)\right)c_{imp}-\left(c^{(0)}\right)_0^j,$$

$c_N^{j+1}=\left(2hd^{c,j}-c_{N-2}^{j+1}+4c_{N-1}^{j+1}\right)/3$ where $d^{c,j}$ is calculated according to (19) and $j=0,1,\ldots M-1$. From the first of equations (16) and equation (17), it follows that

$c_i^0=\left(1-f_\theta\left(\alpha_0\left(-\varepsilon+i\cdot h\right)\right)\right)\cdot c_{imp}-\left(c^{(0)}\right)_i^0$ where

$i=\overline{0,N_1}$. Having found the values of the concentration on time layer $j+1$, we find the values of the pore fluid pressure on this layer, solving the following system of equations in finite differences obtained by discretization of equations (3), (4), (6), and (8). In this work we use the following discretization of (3)

$$m\beta_p\left(p_i^{j+1}-p_i^j\right)/\tau+\sigma Z_i^j\left(p_{i+1}^{j+1}-p_{i-1}^{j+1}\right)/2/h-\sigma_2\Lambda_i^{p,j+1}K/\tilde{\mu}_i^{j+1}=g_i^j \quad (20)$$

where $Z_i^j=m\beta_p\tilde{V}_i^j-K\left(1/\tilde{\mu}_{i+1}^{j+1}-1/\tilde{\mu}_{i-1}^{j+1}\right)/2/h$,

$$\tilde{V}_i^j=-K\left(\left(p_{i+1}^j-p_{i-1}^j\right)/2/h+\left(\partial p^{(0)}/\partial x\right)_i^j+\rho g\right)/\tilde{\mu}_i^{j+1}$$

$$,\ \tilde{\mu}_i^{j+1}=\left(\mu_g-\mu_w\right)\left(c_i^{j+1}+\left(c^{(0)}\right)_i^j\right)+\mu_w,$$

$$\Lambda_i^{p,j+1}=\left(p_{i+1}^{j+1}-2p_i^{j+1}+p_{i-1}^{j+1}\right)/h^2,$$

$$g_i^j=-m\beta_p\left(\partial p^{(0)}/\partial t\right)_i^j-Z_i^j\left(\partial p^{(0)}/\partial x\right)_i^j+K/\tilde{\mu}_i^{j+1}\left(\partial^2 p^{(0)}/\partial x^2\right)_i^j-\Xi_i^j, \quad (21)$$

$$\Xi_i^j=\left(1-\sigma\right)Z_i^j\frac{p_{i+1}^j-p_{i-1}^j}{2h}-\frac{K\left(1-\sigma_2\right)\left(p_{i+1}^j-2p_i^j+p_{i-1}^j\right)}{\tilde{\mu}_i^{j+1}\quad h^2}-\frac{K\rho g}{2h}\left(\frac{1}{\tilde{\mu}_{i+1}^{j+1}}-\frac{1}{\tilde{\mu}_{i-1}^{j+1}}\right),$$

and the following discretizations of equations (4), (6), and (8)

$$p_i^0=\hat{p}_i,\quad \left(-p_2^{j+1}+4p_1^{j+1}-3p_0^{j+1}\right)/2/h=d^{p,j},\ p_N^{j+1}=\tilde{p}^j \quad (22)$$

where

$$g_\theta\left(\alpha_1\varepsilon\right)=\left(1-f_\theta\left(\alpha_1 x\right)-x df_\theta\left(\alpha_1 x\right)/dx\right)\Big|_{x=-\varepsilon}$$

$$d^{p,j}=-\mu_1 mV_0 g_\theta\left(\alpha_1\varepsilon\right)/K-\rho\cdot g-\left(dp^{(0)}/dx\right)_0^j, \quad (23)$$

$$\tilde{p}^j=\left(f_\theta\left(\alpha_1 L\right)-1\right)L\mu_1 mV_0/K-\left(p^{(0)}\right)_{N_1}^j, \quad (24)$$

$$\hat{p}_i=\rho g\left(L+\varepsilon-i\cdot h\right)+\mu_1 q_{1inp}\left(-\varepsilon+i\cdot h\right)\left(f_\theta\left(\alpha_1\left(-\varepsilon+i\cdot h\right)\right)-1\right)/S/K-\left(p^{(0)}\right)_i^0. \quad (25)$$

In (20), (22) $i=1,2,\ldots N-1$, $j=0,1,\ldots M-1$. If $\sigma_2\neq 0$, then the system of equations (20), (22) in finite differences can be solved by the "progonka" method. Thus, using known values of the pore fluid pressure in nodal points on time layer j and known values of the cement concentration in nodal points on time layers j and $j+1$, we can calculate the pore fluid pressure in nodal points on time layer $j+1$. In its turn, using known values of the pore fluid pressure and the cement concentration in nodal points on time layer j we can calculate such the values on time layer $j+1$. Since these values on the zero time layer can be found from the first equations of ones (16) and (22), we can find space distributions of the pore fluid pressure and the cement concentration on any time layer. Constants σ, σ_1, and σ_2 are introduced in (14), (20) to have an opportunity during a numerical solution analysis to estimate the round off error and to check whether the replacement of derivatives in problem (2)–(9) with their finite difference analogs is not ill-posed.

An Analysis of Numerical Solutions. An analysis of the cement concentration and the pore fluid pressure distributions in the pore medium at moments of time $t=100$ sec, $t=250$ sec, and $t=400$ sec obtained numerically is performed according to the following scheme. We assign specific values to all input parameters. In what follows, this set of input parameters is called the main set. To estimate an uncertainty in the value of the cement concentration (the pore fluid pressure) due to an uncertainty in a chosen input parameter, we calculate the distribution of this value first using the main input parameter set and then using the input parameter set distinct from the main set by the value of the chosen parameter. The difference between the assigned value to the chosen parameter and the respective value in the main set characterizes the degree of the uncertainty of the chosen parameter value. The measure of a difference between obtained distributions calculated according to the first of equations (12) gives the sought estimation. We distinguish two types of input parameters. Parameters of the first type are determined by the calculation method, where as parameters of the second one are determined by laboratory measurements. The second type parameter values from the main set and their absolute errors are presented in Table 1. These errors are determined from the last significant digits in values of these parameters [4, p. 41]. In the case of the main set, the pore fluid pressure and cement concentration distributions in the pore medium are calculated by the second method and using such space and time increments $h=\left(0,7+\varepsilon\right)/500$ m, $\tau=0,005$ sec respectively. We assume (assumption #4) that the shape of function $f_\theta\left(\alpha\cdot x\right)$ does not influence significantly the calculated distributions. In the main set, this shape is determined by the following function

$$f_\theta\left(\alpha\cdot x\right)=0,5+arctg\left(\alpha\cdot x\right)/\pi. \quad (26)$$

In our model, ε is a small parameter, while α_0 and α_1 are large parameters, and, therefore, in the main set, we assign to them such values

$$\varepsilon=1,0\times 10^{-3}L/N,\ \alpha_0=5\cdot 10^3/\varepsilon tg\left(\pi\left(0,5-1/e^2\right)\right),\ \alpha_1=\alpha_0 \quad (27)$$

where $N=500$. In this set, constants σ, σ_1, σ_2, V_{eff}, and μ_{eff} have the following values $\sigma=\sigma_1=\sigma_2=1$, $\mu_{eff}=\left(\mu_1+\mu_2\right)/2$, and $V_{eff}=\left(V_0+V_1\right)/2$. From (13) and (26) it follows that $\alpha_c=tg\left(\pi\left(0,5-1/e^r\right)\right)/8/a_L$. To choose the value of α_c the calculations are performed varying r from 0,7 to 2,5 with the increment $\Delta r_1=0,2$ and from 2,5

to 4,5 with the increment $\Delta r_2 = 0{,}1$. The dependencies of $\varepsilon_2^c/\varepsilon_1^c$ and $\varepsilon_2^p/\varepsilon_1^p$ on r are presented on Figures 1 (a) and 1 (b). They are calculated by using

Table 1. **The Values of the Second Type Parameters and Their Absolute Errors**

Parameter	Parameter Value	Absolute Error
Porosity	0,335	0,0005
Grout density	1370 *kg/m³*	5 *kg/m³*
Grout viscosity	2,9·10⁻³ *Pa·sec*	5·10⁻⁵ *Pa·sec*
Intrinsic permeability	1,17·10⁻¹¹ *m²*	5·10⁻¹⁴ *m²*
Diffusion coefficient	1,.0·10⁻¹⁰ *m²/sec*	5·10⁻¹² *m²/sec*
Longitudinal dispersion coefficient	2,0·10⁻² *m*	5·10⁻⁴ *m*
Compressibility coefficient	3,0·10⁻⁸ *Pa⁻¹*	5·10⁻¹⁰ *Pa⁻¹*
Water viscosity	1,1·10⁻³ *Pa·sec*	5·10⁻⁵ *Pa·sec*
Pumping rate	1,5·10⁻⁶ *m³/sec*	5·10⁻⁸ *m³/sec*
Tube length	0,70 *m*	5·10⁻³ *m*
Tube diameter	0,08 *m*	5·10⁻³ *m*
Acceleration of free fall	9,8 *m/sec²*	0,05 *m/sec²*

input parameter values except for the value of r from the main set. Lines 1, 2, and 3 on these figures correspond to the moments of time $t = 100$ sec, $t = 250$ sec, and $t = 400$ sec respectively. Table 2 contains the values of r at which these lines reach their maximums on segment $[0{,}2\ \ 4{,}5]$. The fact that these maximums exist verifies assumption #1. In this table, $r_{\max}^c$ corresponds to the lines from Figure 1 (a) and $r_{\max}^p$ corresponds to the lines from Figure 1 (b). Since in all cases presented in Table 2 $\Delta r_1, \Delta r_2 << \left| r_{\max}^c - r_{\max}^p \right|$, the values of Δr_1 and Δr_2 are sufficiently small. The distribution of the concentration (the pressure) obtained numerically with the usage of the main set of input data being compared with the rest of distributions of the concentration (the pressure) obtained numerically during the numerical solution analysis is interpolated by the local spline that is most interesting for applications [3, p. 34–38]. We assume (assumption #5) that the results of numerical anal-

Table 2. **Values of r at which ratios $\varepsilon_2^c/\varepsilon_1^c$ and $\varepsilon_2^p/\varepsilon_1^p$ calculated for the moments of time $t = 100$ *sec*, $t = 250$ *sec*, and $t = 400$ *sec* reach their maximal values**

	$t = 100$ *sec*	$t = 250$ *sec*	$t = 400$ *sec*
$r_{\max}^c$	2,7	2,3	1,9
$r_{\max}^p$	1,5	4,1	3,9

yses of distributions of the concentration (the pressure) at the chosen moments of time do not depend upon a choice of a type of a spline used for the interpolation. Between the estimations of uncertainties in the cement concentration (the pore fluid pressure) at each chosen moment of time and at any point inside the tube due to uncertainties in the first type parameter values the largest ones are the uncertainties due to uncertainties in the space coordinate grid increment, the choice of the calculation method, and value of α_c. In its turn, between the estimations of uncertainties in the cement concentration (the pore fluid pressure) at each chosen moment of time and at any point inside the tube due to uncertainties in the second type parameter values the largest ones are the uncertainties due to uncertainties in the pumping rate and the diameter of the tube. In what follows we denote them respectively as ε_i^c $\left(\varepsilon_i^p\right)$ where $i = \overline{1,5}$ and upper index c (p) corresponds to cement concentration (pore fluid pressure). Their values are given in Table 3. The fact that the total trancation errors of the cement concentration and the pore fluid pressure at the chosen moments of time and at any point inside the tube can be estimated as $\tilde{\varepsilon}^c = \sqrt{\sum_{i=1}^{3}\left(\varepsilon_i^c\right)^2}$, $\tilde{\varepsilon}^p = \sqrt{\sum_{i=1}^{3}\left(\varepsilon_i^p\right)^2}$ verifies assumption # j where $j = \overline{2,5}$ [4, p. 67]. $\hat{\varepsilon}^c$ and $\hat{\varepsilon}^p$ that are given in Table 3 are estimations of total errors. First, they are calculated as the square roots of the sums of squares of estimations of uncertainties in respective values at chosen moments of time and at any point inside the tube due to uncertainties in all input parameters. Then, they are rounded off according to the rule of error rounding off [4, p. 26]. Sound transducers c_1, c_2, and c_3 placed respectively at distances from the injection point *0,2 m*, *0,4 m*, and *0,6 m* detect the grout front at moments of time $t_1 = 100$ sec, $t_2 = 250$ sec, and $t_3 = 400$ sec respectively [8, p. 80]. The values of the concentration at points $x = 0{,}2$ *m*, $x = 0{,}4$ *m*, and $x = 0{,}6$ *m* at these moments of time are the following:

$$c(x = 0{,}2 \text{ m}, t_1) = 60 \pm 120 \ kg/m^3,$$

$$c(x = 0{,}4 \ m, t_2) = 60 \pm 170 \ kg/m^3,$$

$$c(x = 0{,}6 \ m, t_3) = 40 \pm 200 \ kg/m^3.$$

Their error bars are taken from Table 3. The fact that these values coincide within error limits means that the results of laboratory measurements do not contradict to the results of numerical calculations. However, since the numerical errors are significant, this fact provides a small amount of information [2, p. 46-47]. The

Table 3. **The uncertainties of the distributions of the cement concentration and pore fluid pressure at chosen moments of time due to uncertainties in the input data of the first type in units kg/m³ and Pa respectively**

	100 *sec*	250 *sec*	400 *sec*		100 *sec*	250 *sec*	400 *sec*
ε_1^c, *kg/m³*	0,653	0,319	0,166	ε_1^p, Pa	3,358	2,236	1,704
ε_2^c, *kg/m³*	0,246	0,135	0,074	ε_2^p, *Pa*	1,340	0,572	0,399
ε_3^c, *kg/m³*	0,222	1,452	1,069	ε_3^p, *Pa*	0,753	2,582	2,223
$\tilde{\varepsilon}^c$, *kg/m³*	0,772	1,50	1,09	$\tilde{\varepsilon}^p$, *Pa*	3,93	3,68	3,03
ε_4^c, *kg/m³*	31,7	46,0	56,7	ε_4^p, *Pa*	964	1379	1793
ε_5^c, *kg/m³*	113,7	164,0	201,4	ε_5^p, *Pa*	3234	4553	5871
$\hat{\varepsilon}^c$, *kg/m³*	120	170	200	$\hat{\varepsilon}^p$, *Pa*	3000	5000	6000

fact that in each considered case $\tilde{\varepsilon}^c << \hat{\varepsilon}^c$, $\tilde{\varepsilon}^p << \hat{\varepsilon}^p$ indicates that the trancation method and round off errors are negligible in comparison with the error due to uncertainties in the second type input data in all considered cases. Therefore, we calculate the dependence of the injection pressure upon the time using the first method and the implicit differential scheme. The scheme of the analysis of numerical dependencies of the injection pressure upon the time differs from the scheme of the analysis of numerical distributions of the concentration and the pressure at the chosen moments of time in the following ways. The dependencies of the injection pressure upon the time are compared according to the second of equations (12). In this analysis the main set of input data differs from the one of the previous analysis by the fact that calculations are performed by the first method and the injection time is equal to 800 *sec*. Besides, since the calculations are performed by using the rather small time increment, the numerical dependence of the injection pressure upon the time is reconstructed between the nodal points by the piece-wise quadratic interpolation during this analysis. Between the estimations of uncertainties in the dependence of injection pressure upon time due to uncertainties in the input parameter values the largest ones are the uncertainties due to uncertainties in the pumping rate and the diameter of the tube. They have such values $\omega_1 = 2175$ Pa and $\omega_2 = 7438$ Pa respectively. The total error in this case, first, is calculated as the square root of the sum of squares of estimations of uncertainties in injection pressure at any moment of time due to uncertainties in all input parameters. Then, it is rounded off according to the rule of error rounding off [4, p. 26]. It has such the value $\hat{\omega} = 7860$ Pa. The error bars of the numerical injection pressure evolution are presented on Figure 1 (c). The experimental dependence of the injection pressure on time is presented in paper [8, p. 81]. It coincides within error bars with the numerical one shown on Figure 1 (c). Since the numerical error as well as the experimental one is significant, such the comparison provides a small amount of information too [2, p. 46–47].

Conclusions. Thus, in all considered cases the main contribution to the total error comes from the uncertainty in the calculated value due to the uncertainty in the diameter of the tube. In papers [6, p. 1215–1216], [7, p. 230] the standard laboratory

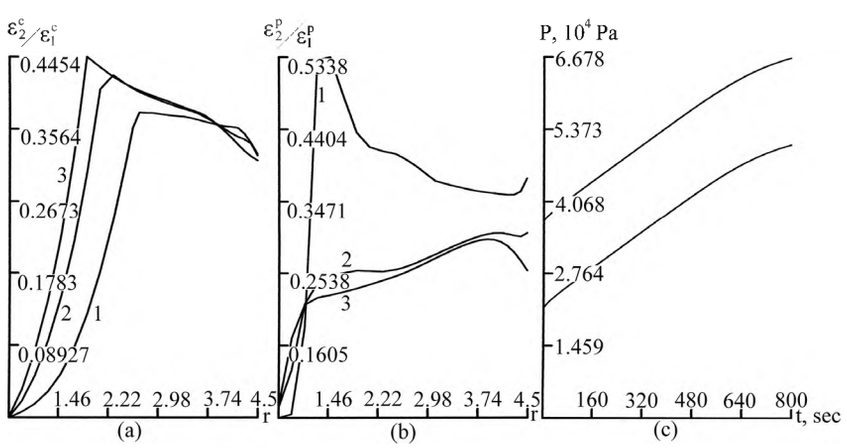

Fig. 1. *a, b* – The dependences of $\varepsilon_2^c/\varepsilon_1^c$ and $\varepsilon_2^p/\varepsilon_1^p$ on r: 1 – $t = 100$ *sec*, 2 – $t = 250$ *sec*, 3 – $t = 400$ *sec*; *c* – The error bars of numerical injection pressure evolution

investigation same as in this one was modeled and the tube diameters were equal to $0{,}07 \pm 0{,}005$ m and $0{,}1 \pm 0{,}05$ m respectively. Since in the test discussed in this work the tube diameter is equal to $0{,}08 \pm 0{,}005$ m, we can conclude that, in recent research [6], [7] as well as in this paper, the comparison of model calculations with results of laboratory measurements provides a small amount of information. Consequently, the attention should be paid to the precision of laboratory measurements.

References

1. Власюк А. П. Застосування числових конформних відображень до розв'язання крайової задачі з рухомою межею для рівняння параболічного типу у криволінійному чотирикутнику / А. П. Власюк, М. Б. Демчук, М. М. Обезюк // Вісн. Нац. ун-ту водн. госп-ва та природокористув. – 2007. – Вип. 4 (40). – Ч. 3. – С. 268–286.
2. Демчук М. Б. Узгоджена модель нагнітання цементного розчину в насичене пористе середовище / М. Б. Демчук // Наукові записки НАУКМА. – 2011. – Т. 125. Комп'ютерні науки. – С. 46–51.
3. Рябенький В. С. Введение в вычислительную математику : учебное пособие / В. С. Рябенький. – М. : Физматлит, 2000. – 294 с.
4. Тейлор Дж. Введение в теорию ошибок / Дж. Тейлор – М. : Мир, 1985. – 272 с.
5. Федоренко Р. П. Введение в вычислительную физику / Р. П. Федоренко. – М. : Издательство Московского физико-технического института, 1994. – 526 с.
6. Bouchelaghem F. Mathematical and numerical filtration-advection-dispersion model of miscible grout propagation in saturated porous media / F. Bouchelaghem, L. Vulliet // International journal for numerical and analytical methods in Geomechanics. – 2001. – Vol. 25, № 12. – P. 1195–1227.
7. Chupin O. The effects of filtration on the injection of cement-based grouts in sand columns / O. Chupin, N. Saiyouri, P.-Y. Hicher // Transport in porous media. – 2008. – Vol. 72, № 2. – P. 227–240.
8. Demchuk M. B. A realization of the uncertainty uniformity principle in a grouting model / M. B. Demchuk, N. Saiyouri // Математичне та комп'ютерне моделювання : зб. наук. пр. Сер. фіз.-мат. науки, 2012. – Вип. 7. – С. 77–92.
9. Sharma M. M. Transport of particulate suspensions in porous media: model formulation / M. M. Sharma, Y. C. Yortsos // American Institute of Chemical Engineers Journal, 1987. – Vol. 33, № 10. – P. 1636–1643.

Демчук М. Б.

ОБҐРУНТУВАННЯ МОДЕЛЕЙ ЦЕМЕНТАЦІЇ ҐРУНТІВ

Оцінено похибки числових розрахунків згідно з моделлю стандартного лабораторного дослідження нагнітання цементного розчину в насичене пористе середовище. У такому дослідженні обґрунтовуються модельні припущення, порівнюючи результати модельних розрахунків із результатами відповідних лабораторних вимірювань. Показано, що обґрунтування, представлене в даній роботі, а також обґрунтування, представлені у недавніх подібних дослідженнях цього процесу, є малоінформативними.

Ключові слова: непокращувана похибка, похибка методу, похибка заокруглення, аналіз числових розв'язків, принцип рівномірності похибки.

Матеріал надійшов 14.02.2013